## Title

Methods for determining equiluminance in terms of L/M cone ratios.



## Journal

Journal of Vision, 20(4)

## Authors

He, Jingyi
Taveras Cruz, Yesenia
Eskew, Rhea

## Publication Date

2020-04-09

## DOI

10.1167/jov.20.4.22

Peer reviewed

# Methods for determining equiluminance in terms of L/M cone ratios

**Jingyi He** Department of Psychology, Northeastern University, Boston, MA, USA

**Yesenia Taveras Cruz** Department of Psychology, Northeastern University, Boston, MA, USA

**Rhea T. Eskew, Jr** Department of Psychology, Northeastern University, Boston, MA, USA

**Heterochromatic flicker photometry (HFP), minimum motion (MM), and minimally distinct border (MDB) settings have often been used to determine equiluminance, a relative intensity setting for two chromaticities that, in theory, eliminates the responses of a luminance or achromatic psychophysical mechanism. These settings have been taken to reflect the relative contribution of the long (L) and medium (M) wavelength cones to luminance, which varies widely across individuals. The present study compares HFP, MM, and MDB using stimuli that do not modulate the short (S) wavelength cones, in both practiced and naïve observers. MDB was performed with both flashed and steadily viewed stimuli. Results are represented in the (ΔL/L, ΔM/M) plane of cone contrast space. Considering both practiced and naïve observers, both MM and HFP had excellent within-subject precision and high test–retest reliability, whereas HFP also had low between-subject variability. The MDB tasks were less reliable and less precise. The mean L:M contrast ratios at equiluminance were lower for the two temporal tasks (HFP and MM) compared to the spatial tasks (MDB), perhaps consistent with the existence of multiple luminance mechanisms. Overall, the results suggest that the best method for determining equiluminance is HFP, with MM being a close second.**

## Introduction

### Luminous efficiency functions *V*(λ)

Photometric luminance was originally defined by the International Commission on Illumination (CIE) using the 1924 $V(\lambda)$ function, which is based on data from several experimental methods (Wyszecki & Stiles, 1982). Proposals to modify the shape of the curve to better agree with psychophysical data, most notably that of Judd (Vos, 1978), eventually led to a "physiologically relevant" CIE standard (CIE, 2006, 2015). One method used to define these $V(\lambda)$ curves was heterochromatic flicker photometry (HFP). In HFP, the observer sets the radiance of each test light to minimize the perceived flicker of the test as it alternates with a standard light; when the tests are monochromatic, the result is a function of wavelength, HFP(λ). The curve reflects the activity of the long (L) and medium (M) wavelength cones with little or no input from the short (S) wavelength cones (Eisner & Macleod, 1981; Smith & Pokorny, 1975), under the measurement conditions that are most commonly employed (Ripamonti, Woo, Crowther, & Stockman, 2009), and the modern standard is modeled as a weighted sum of the Stockman–Sharpe L and M cone fundamentals (Stockman & Sharpe, 2000). Because of the relatively high temporal frequency that is normally used in HFP, the minimization of the sensation of flicker that defines the curve is generally believed to result from minimizing the activity in the magnocellular pathway (Lee, Martin, & Valberg, 1988). However, luminance and chromatic information may be multiplexed in the parvocellular pathway (Ingling & Martinez, 1983; Ingling & Martinez-Uriegas, 1983), and thus there may, in fact, be more than one luminance pathway (for discussion, see Stockman & Brainard, 2010).

### Luminous efficiency represented in cone contrast space

In the present study, stimuli only modulated the L and M cones, with the S cone quantal catch kept constant. We present the results in the (ΔL/L, ΔM/M) plane of cone contrast space (Figure 1b). In this space, each axis represents the modulation or change in cone quantal catch due to a test light (e.g., ΔL) divided

Citation: He, J., Taveras Cruz, Y., & Eskew, R. T., Jr (2020). Methods for determining equiluminance in terms of L/M cone ratios. *Journal of Vision*, *20*(4):22, 1–13, https://doi.org/10.1167/jov.20.4.22.

https://doi.org/10.1167/jov.20.4.22 Received September 11, 2019; published April 28, 2020 ISSN 1534-7362 

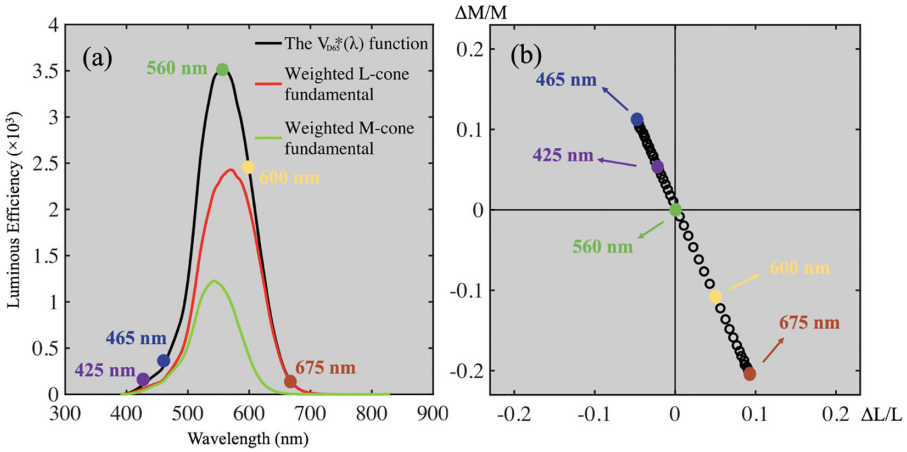


Figure 1. $V(\lambda)$ function and its cone contrast transformation. (a) The $V_{D65}$*(λ) luminous efficiency function of Sharpe et al. (2011), along with its L cone and M cone fundamental components, all as functions of wavelength. The black bell-shaped curve is the $V_{D65}$*(λ) curve. The red and green curves are the L cone and M cone fundamentals, respectively, in energy units. The two weighted fundamentals add up to the $V_{D65}$*(λ). (b) Transformation of $1/V_{D65}$*(λ) values to the (ΔL/L, ΔM/M) plane of cone contrast space, at 5-nm steps, from 425 to 675 nm. Each point represents the (ΔM/M)/(ΔL/L) ratio for a specific wavelength at the flicker null (Eskew et al., 1999; Sharpe et al., 2011). Data were downloaded from http://www.cvrl.org.

by the cone activity produced by the steady lights to which the observer is adapted (L) (Brainard, 1996; Eskew, McLellan, & Giulianini, 1999). Thus, the origin represents the adapting condition, and the increments and decrements in cone activity are represented in the four quadrants of the plane; the second and fourth quadrants (QII and QIV), in which the two cone contrasts have opposite signs, are the focus of attention in this study.

Figure 1 illustrates the relationship between a traditional luminous efficiency curve and its cone contrast representation. In panel (a), we plot the CIE (2006) 2° $V_{D65}$*(λ) luminous efficiency function of Sharpe, Stockman, Jagla, and Jägle (2005) in energy terms, as derived from HFP (Sharpe, Stockman, Jagla, & Jägle, 2011; Stockman, Jagle, Pirzer, & Sharpe, 2008). $V_{D65}$*(λ) is intended to be used for daylight (D65) adapting conditions; the data were corrected for chromatic adaptation to the test lights themselves. The height of the curve represents flicker sensitivity as a function of wavelength, relative to a 560-nm standard light. When the sensitivity curve is inverted, its height is proportional to the radiance required to minimize the flicker of the test light against the standard light (for an average observer). The curve is a sum of the L (red curve) and M (green curve) cone fundamentals, with the L function weighted by 1.98 compared to the M function. Like any HFP(λ) function, $V_{D65}$*(λ) represents *stimuli*.

In contrast, a luminance or achromatic *mechanism* may be modeled as a weighted sum of cone signals (Eskew et al., 1999; Kaiser & Boynton, 1996; Stockman & Brainard, 2010; Stromeyer et al., 2000). Under conditions where the cones adapt independently according to Weber's law, the effect of adaptation may be accounted for by representing the cone signals as contrasts; thus,

$$k_1\frac{\Delta L}{L}+k_2\frac{\Delta M}{M}=\text{Luminance mechanism signal} \quad (1)$$

with $k_1$ and $k_2$ being non-negative weights. When the response is constant, as is believed to be the result of HFP, the equation forms a line in the (ΔL/L, ΔM/M) plane. For simplicity, we assume that the modulation produced in the luminance mechanism is zero at the HFP setting—that is, when the test and standard are equiluminant.

In Figure 1b, the inverses of the sensitivities from the $V_{D65}$*(λ) curve at every 5 nm have been transformed into L and M cone contrasts (assuming fixed adapting conditions and cone-independent, Weberian adaptation[1]); in effect, we have computed the pair of cone contrast values for the test peak of the flicker waveform at different wavelengths of flicker. The cone contrast pairs fall along a line through the origin; this line is parallel to the luminance mechanism threshold line under these same assumptions (Eskew et al., 1999). At equiluminance, test wavelengths shorter than 560 nm produce relatively positive modulations in the M cones and negative modulations in the L cones, and test wavelengths longer than 560 nm produce positive modulations in the L cones and negative modulations in the M cones, at the peak of the flickering waveform, both in reference to the 560-nm standard. The 560-nm light produces zero contrast when it is both test and standard and therefore plots at the origin. The HFP thresholds from $V_{D65}$*(λ) fall along a line of slope –2.23.

As shown in Appendix A, the relative L cone fundamental weight $w$ in an HFP function such as $V_{D65}^*(\lambda)$ is equal to the slope in cone contrast space multiplied by the ratio of the two adapting levels, $M_{adapt}/L_{adapt}$. According to the ideas outlined above, at the HFP setting where the mechanism response is zero,

$$\frac{\Delta M}{M} = -\frac{k_1}{k_2}\frac{\Delta L}{L} = -2.23\frac{\Delta L}{L} \quad (2)$$

As shown in Appendix A, the relative weight ($w$) on the L cone fundamental in $V_{D65}^*(\lambda)$ (Figure 1a) is

$$w = \frac{k_1}{k_2}\frac{M_{adapt}}{L_{adapt}} = 2.23\frac{M_{adapt}}{L_{adapt}} = 1.98 \quad (3)$$

Under the stated (rather restrictive) conditions, the relative adaptive states determine the relative contribution of the L and M cones to this HFP function, as also shown by Stockman et al. (2008) using a different approach.

In addition to using HFP to model the relative L/M inputs to luminance mechanisms, HFP settings have been taken as indicating the relative numbers of L and M cones in the retina (Gunther & Dobkins, 2002; Kremers et al., 2000; Rushton & Baker, 1964). This latter interpretation is complicated, as the relative L-to-M input to HFP—and thus the given luminous efficiency function $V(\lambda)$—is altered by chromatic adaptation (Eisner & Macleod, 1981; Stockman et al., 2008; Stromeyer, Cole, & Kronauer, 1987), and obviously the cone numbers are not (for discussion, see Stockman & Sharpe, 2000). However, if the adapting conditions are held constant—something that is not the case in conventional HFP studies with monochromatic lights (Stockman et al., 2008)—then the relative weighting of L-to-M fundamentals $w$ might be *proportional* to the relative cone numbers. The relative *cone contrast* weight $k_1/k_2$ might be more directly related to relative cone numbers, as the contrast calculation approximately accounts for adaptation.

### Current study

For all the reasons discussed above, the determination of luminance sensitivity is potentially important. Various methods have been used and compared previously (see, for example, Koenderink, van Doorn, & Gegenfurtner, 2018; Lennie, Pokorny, & Smith, 1993; Stockman & Brainard, 2010; Wagner & Boynton, 1972). The current study compares four different methods for setting equiluminance in both practiced and naïve observers, with the primary goal of the study being to select the most precise and reliable method for use with modern stimulus generation technology and minimizing changes in chromatic adaptation due to the stimuli (see the section on effects of adaptational changes). Overall, HFP and minimum motion (MM) proved to be the best methods, and there were intriguing suggestions of differences between the temporal tasks (HFP and MM) and the spatial tasks (minimally distinct border [MDB]).

## Methods

### Observers

Two groups of observers participated in this study. Twenty-two participants were undergraduate students from Northeastern University who received course credit for their participation. These observers were naïve, having had no prior psychophysical experience and no knowledge of the theory underlying the experiment. All of these observers reported having normal color vision. The second group consisted of four practiced observers, all of whom were experienced with psychophysical observation and also knowledgeable about the experimental hypotheses and background. The experienced observers had normal scores on the Farnsworth–Munsell 100-hue test (Farnsworth, 1943), normal performance on the Ishihara plates, and normal Rayleigh match settings on a Nagel anomaloscope.

This study was approved by the Northeastern University Institutional Review Board. All procedures followed the principles in the Declaration of Helsinki. Informed consent was provided by all observers.

### Apparatus

Stimuli presentation was performed using an Apple Mac computer (Cupertino, CA) running a Bits# display controller (Cambridge Research Systems, Rochester, UK), which drove a Sony GDM-F520 CRT monitor (Tokyo, Japan) at an 85-Hz frame rate. Experimental software was written in MATLAB (MathWorks, Natick, MA) using the Psychtoolbox (Kleiner, Brainard, & Pelli, 2007).

The experiment was conducted in a dark room. Head position was stabilized using a chin rest, at a distance of 130 cm from the screen. A 4.9° black X, with its central 3.4° (diagonal) blank, guided fixation in all experiments. Experienced observers viewed the stimulus monocularly by their dominant eye through ophthalmic trial lenses, with the other eye patched. Naïve participants viewed the screen binocularly and wore their own corrective eyewear.

The monitor spectra were carefully calibrated with a Photo Research PR-650 spectroradiometer (Photo Research, Chatsworth, CA), and gamma correction was achieved by loading in a look-up table to the Bits#. Luminance of the mid-gray ($x = 0.289$, $y = 0.315$) background was 75 cd/m$^2$ (approximately

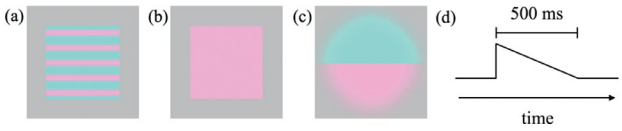


Figure 2. Stimuli. (a)–(c) The 3 × 3° central region of the display. All of the stimuli had two peak chromaticities that were symmetric around the origin in the ΔL/L, ΔM/M plane. (a) MM stimulus. A square patch of 2 × 2°, filled with the superposition of two quadrature gratings of 2.5 cpd, each contrast reversing at 2 Hz. (b) HFP stimulus. A square patch of 2 × 2°, flickering at 10.63 Hz. (c) MDB stimulus. An isolated edge (McLellan et al., 1994) consists of a horizontal edge multiplied by a Gaussian with $\sigma$ =1°. (d) Time course for the flashed stimulus in MDB1 is a rapid-start sawtooth temporal profile; all of the other stimuli, including the MDB2 stimulus which had the same spatial profile as the MDB1 stimulus, were steadily viewed.

2.6 log Td). Temporal frequency of the flickering stimuli was calibrated by an oscilloscope driven by a fast photocell.

## Tasks and stimuli

Four different tasks were performed by each observer, each at two levels of stimulus contrast (Figure 2). For the MM task (Anstis & Cavanagh, 1983; Cavanagh, MacLeod, & Anstis, 1987), a 2° square patch was filled with the superposition of two 2.5-cycles/degree (cpd) horizontal gratings, a chromatic grating (chromaticity in the L/M plane) and an achromatic grating (black and white). These gratings were superimposed and displaced by a quarter cycle vertically and flickered at 2 Hz to create motion (i.e., the bars moved either upward or downward) (Figure 2a). When the two color components of the chromatic grating have input equal to the motion mechanism—presumably a luminance input—the perceived motion is eliminated, and the net result is a counterphase flickering grating. When the luminance component of one chromaticity is stronger than the other, upward or downward motion is perceived. Observers adjusted the stimulus chromaticity (as described below) to minimize the sensation of motion, leaving predominantly or only a flickering percept.

For the HFP task (Ives, 1912), a 2° square spot was sine-wave flickered between two complementary color directions at 10.63 Hz (Figure 2b). Observers adjusted the stimulus chromaticity to minimize the sensation of flicker. The MDB task (Boynton, 1978; Boynton & Kaiser, 1968; Kaiser, Herzberg, & Boynton, 1971) had two variations. The stimulus in both variants was an isolated edge (McLellan, Goodman, & Eskew, 1994), created by multiplying a horizontal step edge by a two-dimensional Gaussian (centered at fixation, with a 1° standard deviation) (Figure 2c). In variant 1 (MDB1), the stimulus was flashed with a sawtooth temporal profile for 500 ms (Figure 2d). The observers' task was to adjust the chromaticity of the two juxtaposed areas to minimize the distinctness of the central edge. A second MDB variation (MDB2) kept the stimulus steady, but the stimulus and task were otherwise the same as for MDB1.

The purpose of using a flashed stimulus for the MDB1 task was to minimize the observer's adaptation to the stimulus itself. Although at the threshold multiples used here there would be some change in the adaptation state during each presentation, there should be less with the flashed MDB1 compared to the steady MDB2. The MM and HFP stimuli modulate rapidly around the mean gray, so presumably they produce relatively little change in the observer's adaptive state as the chromatic angle is adjusted (as noted by Gunther & Dobkins, 2002). Note that the HFP and MM tasks depend strongly on temporal factors, whereas the MDB tasks are primarily spatial.

The HFP and MM stimuli were 2° square, and the two MDB tasks used a Gaussian blob with $\sigma$ = 1°. Stimuli size were kept at around 2° to be able to better compare methods and to match the stimulus size in Sharpe et al. (2011). A moderate temporal frequency (10.63 Hz) for HFP was chosen to reduce S-cone sensitivity (for observers who are not exactly Stockman–Sharpe observers; see next paragraph). The spatial and temporal frequencies used in MM in our experiment were similar to values that have been used in previous studies. Changes in these parameters, especially the temporal frequency in MM, could have produced somewhat different results (Cavanagh et al., 1987).

All of the stimuli were calculated to be constant for S cones (they only modulated L and M) based upon the Stockman–Sharpe cone fundamentals (Stockman & Sharpe, 2000). These fundamentals represent averages across variation in preretinal filtering, effective photopigment optical density, and cone $\lambda_{max}$. Although it is certain that not all of our observers were exactly Stockman–Sharpe observers, and thus our calculated (ΔL/L, ΔM/M) plane does not completely eliminate S cone modulations in all cases, the actual S cone contrasts produced by our stimuli are likely to be low (Smith & Pokorny, 1995). S cone contributions to the tasks used here have been shown to be quite small (Boynton, Eskew, & Olson, 1985; Cavanagh et al., 1987; Smith & Pokorny, 1975), and it is unlikely that our results are much influenced by actual S cone modulation across observers.

In the regions of primary interest in the (ΔL/L, ΔM/M) plane (QII and QIV), the monitor gamut was nearly parallel to the detection contour (Giulianini & Eskew, 1998; Shepard, Swanson, McCarthy, & Eskew,

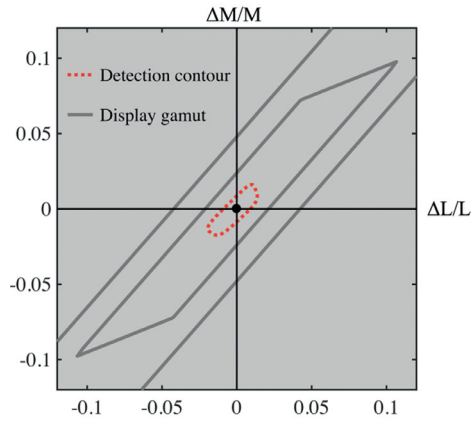


Figure 3. Detection threshold and monitor gamut. (1) The gray lines represent the monitor gamut in the (ΔL/L, ΔM/M) plane at two contrast levels. (2) The red dotted curve is the probability sum fitted to the two-alternative forced-choice (2AFC) detection thresholds from Shepard et al. (2016) for observer TGS, representing the underlying detection mechanisms. The two gamuts are approximately 2.7 and 5.4 times the thresholds in quadrant II.

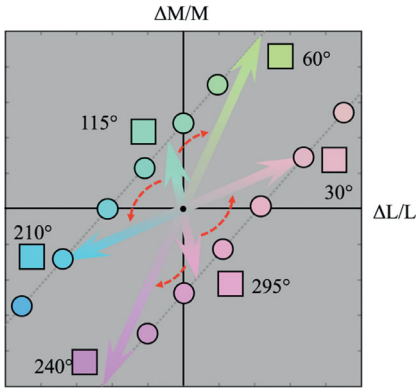


Figure 4. Adjustment procedures. The dotted gray line represents the contrast-scaled monitor gamut in this plane of cone contrast space (see Figure 3). Using HFP as an example, the stimulus flickers between the two chromaticities at 10.63 Hz, as indicated by each of the thick arrows. The angle in the plane was adjusted to increase or decrease the ratio of ΔM/M to ΔL/L of the stimulus. For example, starting from 115° and 295° (flickering between bluish-green and purplish-pink), the observer could reduce the angle and set it to 60° and 240° (flickering between yellowish-green and light purple) or increase the angle and set it to 210° and 30° (flickering between blue and pink). Observers were instructed to find the angle that minimized the sensation of flicker (HFP), motion (MM), or distinctness of the central border (MDB1 and MDB2).

2016), as shown in Figure 3. The stimuli in the present study were always on a contrast-scaled version of the gamut (gray contours in Figure 3) and thus were very nearly a constant multiple of threshold (~2.7 and 5.4 times threshold of observer TGS in Shepard et al., 2016).

In each task, observers adjusted the stimulus chromaticity by the use of three pairs of buttons on a numeric keypad. These buttons altered the color angle of the stimulus in the (ΔL/L, ΔM/M) plane of cone contrast space (i.e., S cones were never modulated), with the three pairs producing large, medium, and small changes in one color rotation direction or its opposite. Figure 4 illustrates the procedure. The two peaks of the stimulus are displayed symmetrically around the origin, which represents the gray of the monitor background. The greenish component is generally in QII, where M cone contrast is positive and L cone contrast is negative, and the reddish component is generally in QIV, where L cone contrast is positive and M cone contrast is negative. Button presses moved the stimulus chromaticity along a line parallel to the gamut of the monitor in this plane of cone contrast space, with the distance of that line from the outer gamut being determined by the contrast: 25% or 50% of the maximum available (gray lines in Figure 3). For a given task and contrast, the observers adjusted the stimulus angle (defined by the chromaticity of the stimulus component on the top half of the cone contrast plane) between 45° and 225° (with the stimulus constrained to lie on the gamut line) for the minimization judgment.

## Procedure

The observers participated in either one or two sessions. The second session occurred at least 1 week after completion of the first one. During each session, four runs (for tasks MM, HFP, MDB1, and MDB2) were completed in random order. Prior to each run, the observers adapted to the gray screen for 60 seconds. Tones were used to signal the end of the adaptation period and the end of each trial. Each run consisted of 10 trials, five at each of the contrast levels (in random order). At the start of the run, the stimulus appeared on the screen with a random color angle. Observers then used the three pairs of keys of different levels of steps to adjust the chromaticity for the given criterion. In the MDB1 task, the stimulus was flashed with the time course shown in Figure 2d when a key was pressed; in all the other tasks, the stimulus was continuously visible.

# Results and discussion

Data of two naïve participants were excluded because they did not follow instructions. Four naïve observers participated in only one session. Therefore, all analyses were done based on four experienced observers

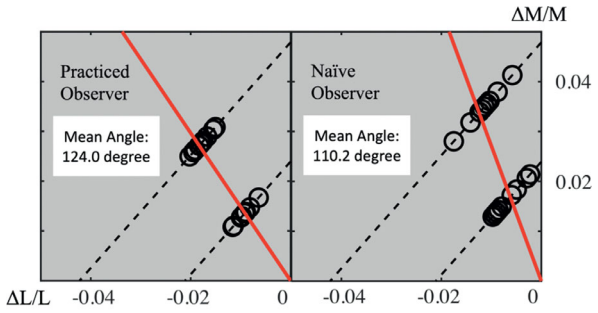


Figure 5. Typical observer scatterplots. Scatterplots of all HFP settings from a typical observer in the two groups, with the red straight line indicating the average equiluminant direction.

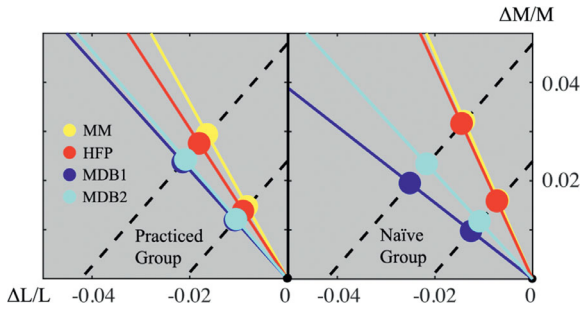


Figure 7. Mean equiluminant directions for practiced and naïve observers (left and right panels, respectively), shown in QII of the cone contrast plane.

and the 14 naïve observers who participated in both sessions. The four naïve observers who completed only one session were excluded from the analysis of test–retest reliability, but their single session data were included in all of the other analyses.

## Data analysis

Each setting results in two redundant cone contrast coordinates: the (ΔL/L, ΔM/M) for each of the two stimulus peaks (Figure 4). The angle between 45° and 225° was used for analysis. An individual's equiluminant angle was calculated as the average of 20 settings (10 settings for the four subjects who completed one session). Two examples in the HFP task are shown in Figure 5, a practiced observer and a naïve observer; each circle is a single setting, and the red line through the origin indicates the average equiluminant direction for this observer. The slope of this line is the average ratio of ΔM/M to ΔL/L at equiluminance. For each observer, we computed a measure of the precision of the settings in each task using the 90% confidence limits on the mean angle.

## Equiluminant angles

All settings are shown in histograms in Figure 6; settings falling in the first quadrant (QI) or third quadrant (QIII) are indicated by angles less than 90° or larger than 180°. Figure 7 illustrates the mean equiluminant directions for each of the four tasks, for the practiced observers in the left panel and the naïve observers in the right, and Table 1 reports the descriptive statistics.

Figure 8 shows the mean angles for the practiced and naïve observers (left two panels) with indications of the variability across observers in mean angle. MM and HFP have the smallest angle (lowest L:M contrast ratio at equiluminance), with MDB1 and MDB2 producing larger angles (higher L:M contrast ratio at equiluminance), especially for the naïve group. The relative L to M contrast weight $k_1/k_2$ (the negative of

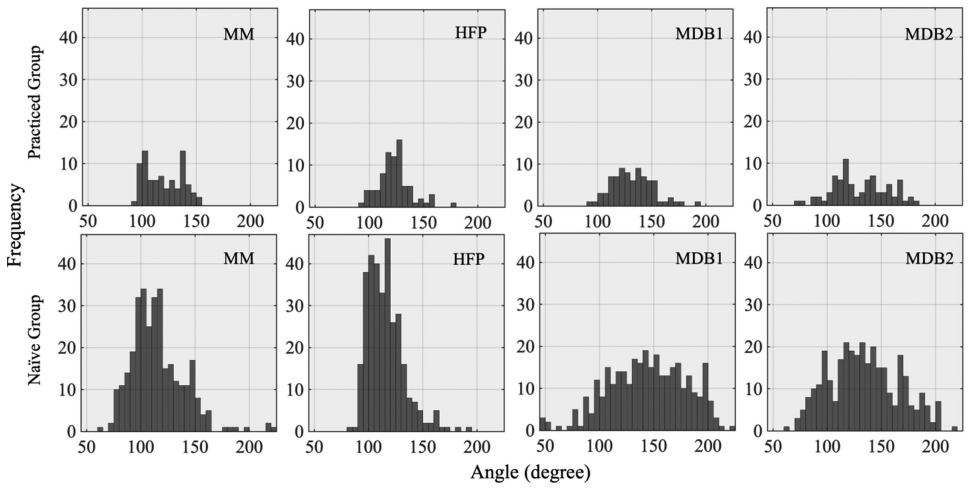


Figure 6. Histograms of all settings. The practiced group is on the top and the naïve group is on the bottom.

| Task | Percent (%) set in QI or QIII | Mean angle (°) | $k_1/k_2$ | 1.645 × SD across observers (°) | Mean of individual 90% CIs (°) |
|---|---|---|---|---|---|
| Practiced group | | | | | |
| MM | 0 | 119.19 | 1.79 | 24.26 | 2.86 |
| HFP | 0 | 123.19 | 1.53 | 16.95 | 3.86 |
| MDB1 | 1.25 | 132.11 | 1.11 | 17.58 | 5.52 |
| MDB2 | 6.25 | 130.75 | 1.16 | 15.61 | 8.23 |
| Naïve group | | | | | |
| MM | 13.75 | 113.53 | 2.30 | 27.53 | 5.33 |
| HFP | 1.25 | 114.73 | 2.17 | 19.43 | 3.86 |
| MDB1 | 23.75 | 142.20 | 0.78 | 30.16 | 10.88 |
| MDB2 | 17.19 | 132.83 | 1.08 | 26.45 | 10.07 |

Table 1. Descriptive results. Percentage of settings made in QI and QIII, mean angle of settings, relative cone contrast weight $k_1/k_2$, 1.645 times standard deviations of the settings across observers, and mean, across observers, of the individual 90% confidence intervals of the settings.

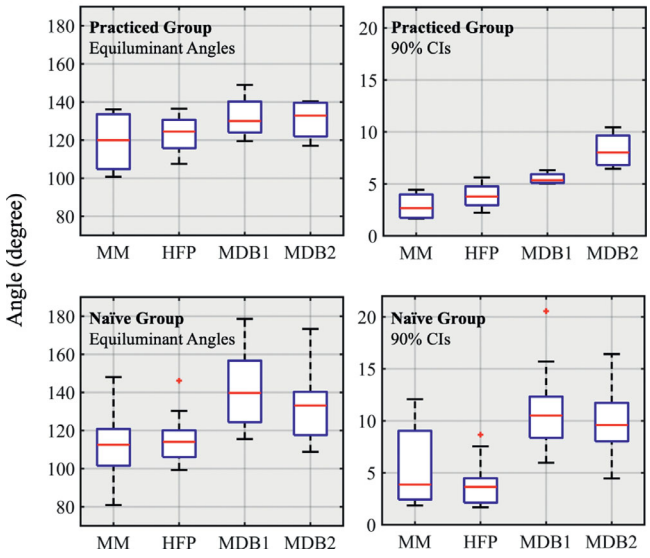


Figure 8. Box and whisker plots of mean angles and 90% confidence intervals. Equiluminant angles (left panels) and within-subject variability (represented by 90% confidence interval; right panels) for practiced (upper panels) and naïve (lower panels) observers. The central red line in each box indicates the median, and the top and bottom ends of the boxes are the 75th and 25th percentile values. The whiskers cover approximately 99.3% of the data, with outliers not included. The outliers are indicated by red plus symbols.

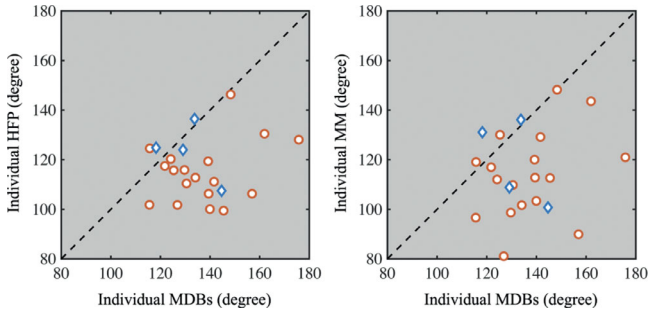


Figure 9. HFP versus MDBs and MM versus MDBs. Each point represents a pair of mean settings of an individual observer. The left panel shows mean HFP settings against (the average of the two sets of) MDB settings, and the right panel plots mean MM settings against (the average of the two sets of) MDB settings. Practiced observer settings are denoted by blue diamonds, and naïve observer settings are shown in red circles. In both figures, the points mostly fall below the dashed line of equality.

the slope; Appendix A), averaged across tasks, was about 1.4 for both groups. For the practiced observers, repeated measure analysis of variance (ANOVA) testing equality of means across the four tasks did not reach conventional significance ($F(3, 9) = 0.797$, $p = 0.53$), probably due to the limited sample size ($n = 4$); for the naïve observers, $F(3, 51) = 21.63$, $p < 0.01$, with least significant difference (LSD) post hoc tests indicating that HFP and MM were different from the two MDBs but not from each other. These differences also hold at the level of the individual observer, not just in the means. As shown in Figure 9, when plotting HFP or MM settings against settings of the average of the two MDB tasks, most of the points fall below the line of equality, indicating that MDB angles are generally larger than HFP or MM angles; the MDB occurs at a larger L:M ratio than the two temporal tasks.

The first column of Table 1 shows the percentage of settings made in QI/QIII, in which the L and M contrasts have the same sign. For the practiced observers, all settings in the MM and the HFP task are in the second quadrant (as in Figures 1b and 7). The L and M cone contrasts at equiluminance have opposite signs as expected for a mechanism that sums cone contrasts (Equation 1). A small fraction of the settings in the MDB tasks is in QI/QIII. For naïve participants, some settings in every task fall in QI (45° to 90°) or QIII

(180° to 225°), with the HFP task having the lowest proportion, only 1.25%.

The right-hand panels in Figure 8 show 90% confidence intervals on the angles (inversely proportional to the precision of the settings); the means are given in Table 1. For the practiced observers, the MDB2 settings were less precise than the others, showing that the observers were inconsistent in their MDB settings when the stimulus was steadily presented. This might be an indication that observers were adapting to the steadily presented stimuli, changing their relative M:L adaptation across settings depending on the starting angle, making the results more variable. The naïve observers were less precise in general and had especially low precision for both MDB tasks; however, HFP had the same average precision for the two groups. Here, the ANOVA for the practiced group did reach conventional significance ($F(3, 9) = 9.27$, $p < 0.01$), with LSD tests indicating that MM had greater precision than MDB2. For the naïve group, $F(3, 51) = 48.68$, $p < 0.01$, and the LSD tests indicated that HFP and MM were more precise than the two MDBs.

Table 1 also shows the between-subject standard deviation multiplied by 1.645 (the *z*-score corresponding to 90% confidence). HFP was most consistent across naïve observers, and MM was least consistent across practiced observers. It is important to note that this consistency may reflect genuine individual differences; thus, low consistency is not necessarily a negative characteristic in these tasks. Individual differences in psychophysical measurements of luminous efficiency are generally large (Gibson & Tyndall, 1923); in Sharpe et al. (2005), the relative L cone weight required to fit HFP(λ) functions varied by a factor of 34 across observers (considering ser180 and ala180 L cone polymorphism observers together). Flicker electroretinogram (ERG)-derived L:M cone contribution ratios varied by a factor of about 32 in one study (Carroll, Neitz, & Neitz, 2002). If we exclude the mean angles that fall outside of QII, the ranges of individual mean angles we found for practiced and naïve observers were 100.8° to 149.0° and 96.5° to 178.6°, respectively, and the corresponding L:M contrast weights ranged from 5.242 to 0.601 and 8.777 to 0.024, with factors of 9 and 366, respectively, combining the data from all tasks. In our HFP results, the average L:M contrast weight $k_1/k_2$ across all participants ($n = 22$) was about 2.0 (and on this measure there was little difference between practiced and naïve participants relative to the variation within these groups) (Figure 8; Table 1). Sharpe et al. (2011) reported that their mean L:M weight in HFP was 2.67 ($n = 40$). This variation across studies and across individuals must include individual differences in preretinal filtering, effective cone optical density, and cone $\lambda_{max}$, and perhaps as well as in L:M cone numbers.

| Tasks | Practiced, *r* (*p*) | Naïve, *r* (*p*) |
|---|---|---|
| MM | 0.97 (0.03) | 0.72 (0.00) |
| HFP | 0.96 (0.05) | 0.91 (0.00) |
| MDB1 | 0.51 (0.49) | 0.45 (0.11) |
| MDB2 | –0.03 (0.97) | 0.73 (0.00) |

Table 2. Test–retest reliability, where *r* is the Pearson correlation.

| Task | MM | HFP | MDB1 | MDB2 |
|---|---|---|---|---|
| Practiced group, *r* (*p*) | | | | |
| MM | — | | | |
| HFP | 0.86 (0.14) | — | | |
| MDB1 | –0.81 (0.19) | –0.75 (0.25) | — | |
| MDB2 | –0.28 (0.72) | –0.17 (0.83) | 0.76 (0.24) | — |
| Naïve group, *r* (*p*) | | | | |
| MM | — | | | |
| HFP | 0.76 (0.00) | — | | |
| MDB1 | 0.15 (0.55) | 0.14 (0.58) | — | |
| MDB2 | 0.44 (0.07) | 0.41 (0.09) | 0.62 (0.01) | — |

Table 3. Inter-task correlation matrix, where *r* is the Pearson correlation.

## Inter-method consistency and test–retest reliability

Test–retest reliability was determined for observers who participated in both sessions, and the correlation coefficients are shown in Table 2. In the MM and HFP task, practiced observers show reliable settings across sessions; the correlations for MDB1 and MDB2 are not statistically different from zero. For the naïve group, the flicker photometry task has the highest reliability, and MM and MDB2 have good reliability. Intercorrelations among the tasks are reported in Table 3. Overall, the practiced observers show good agreement between MM and HFP tasks and between the two MDB tasks. The correlations between MM/HFP and MDB1/MDB2 are *negative*, suggesting disagreements between observer variation in the temporal tasks and the spatial tasks. However, these correlations are not statistically significant. For the naïve observers, all of the intercorrelations are positive. Like the practiced observers, the two temporal tasks (MM and HFP) are well correlated, as are the two spatial tasks (MDB1 and MDB2), but the temporal and spatial tasks are only weakly correlated, perhaps consistent with the negative intercorrelations for the practiced observers. These negative intercorrelations by the practiced observers may be worth further study, suggesting that perhaps the different methods of setting equiluminance may actually be tapping different systems.

### Effects of adaptational changes

It is very well established that HFP(λ) functions change shape under different steady adaptation conditions (Eisner & Macleod, 1981; Stockman, MacLeod, & Vivien, 1993). Stockman et al. (2008) dealt with the more difficult issue of adaptation to the test lights themselves, which alters relative L/M input across settings, even when the tests are fairly close to threshold (an effect corrected for in the $V_{D65}$*(λ) function of Figure 1). The stimuli used in our MDB tasks are highly likely to alter the adaptation state of the observer as the adjustment was being made (as in most prior MDB studies; see Ingling et al., 1978), with the adaptational effect being perhaps smaller in the flashed MDB1 compared to the steady MDB2. This difference between the two MDB tasks might be consistent with the result that the precision of MDB1 is better than that of MDB2 for the practiced group (Figure 8, upper right panel; Table 1, rightmost column).

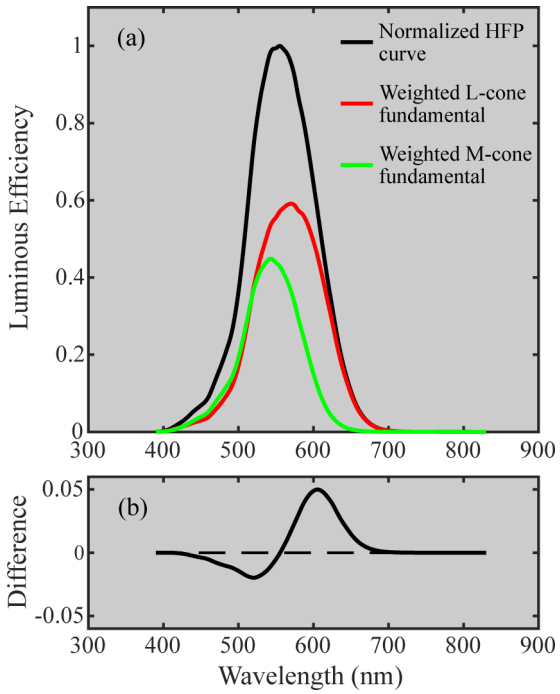


Figure 10. HFP(λ) transformation of the cone-contrast equiluminant direction. (a) The mean HFP equiluminant direction of the practiced group is transformed and plotted in this figure. Compared to Figure 1a, the peak of this reconstructed curve is normalized to 1, and the $V_{D65}$*(λ) curve in Figure 1a is scaled to a real unit. (b) Differences between the normalized $V_{D65}$*(λ) (Figure 1a) and our reconstructed HFP(λ). The vertical axis scale in the lower panel is expanded by about 11 times compared to the upper panel.

## General discussion and conclusions

Of all the tasks, HFP produced the smallest proportion of settings in QI or QIII (Table 1); nearly all of the HFP settings produced L and M cone modulations of opposite sign, as expected for a mechanism that sums cone signals. In addition, naïve observers informally reported that HFP was the easiest task (and MDB was the hardest). The MM task shows good precision and moderate reliability; however, some participants reported that the MM stimulus was uncomfortable to view. This might have been due to our use of four diagonal lines to guide fixation. Those lines might have been insufficient to control eye movements in this task for the naïve observers, perhaps contributing to the discomfort; a small central dot might have been better.

The MDB tasks differ from HFP and MM in at least two important ways. First, the critical feature of the stimulus in MDB (the border itself) is likely to be centrally fixated by the observer, in comparison to the larger HFP and MM stimuli. Thus, retinal inhomogeneities (especially higher macular pigment density and higher cone photopigment optical density in central fovea) might contribute to differences between MDB and HFP/MM. The second difference is that the MDB tasks are primarily spatial, in contrast to the temporal HFP and MM tasks. One might therefore speculate that MDB might depend upon the multiplexed luminance signal in parvocellular neurons (Ingling & Martinez, 1983; Ingling & Martinez-Uriegas, 1983), whereas the temporal tasks could depend upon magnocellular activity (Lee et al., 1988). If this were the case, our results would suggest that, on average, near-foveal magnocellular cells would receive relatively stronger L cone input than parvocellular cells, as both our naïve and practiced observers required greater M cone contrasts to produce equiluminance in the temporal tasks compared to the MDB (Figure 7; Table 1). However, complicating this interpretation of a magnocellular substrate for HFP and MM and a parvocellular substrate for MDB is the fact that MDB settings are undisturbed by moderate amounts of blur (Lindsey & Teller, 1989)—high acuity is not required—and, more to the point, the claim that magnocellular activity can account for MDB settings (Kaiser, Lee, Martin, & Valberg, 1990). Nonetheless, this difference between spatial and temporal luminance tasks is worth further exploration, as are the effects of retinal inhomogeneity.

In Figure 10a, we reconstruct an HFP(λ) based upon the mean of our practiced observers and our $M_{adapt}/L_{adapt}$ ratio of 0.86, with the relative L cone fundamental weight being 1.32; compare this figure to Figure 1a, which has a relative L cone fundamental weight of 1.98. This curve is the prediction, based upon our results, of the HFP using monochromatic lights,

assuming the observer's adaptation state did not change with test wavelength (or that the data were corrected for that change in adaptation) (Stockman et al., 2008). Figure 10b shows the difference between the normalized $V_{D65}$*(λ) of Figure 1 and our reconstructed HFP(λ) in the top panel, as a function of wavelength. The differences are very small but are of course systematic.

For our stimulus conditions, and considering practiced and naïve observers together, heterochromatic flicker photometry proved to be the best method, in terms of its within-subject precision and high test–retest reliability across groups. The minimum motion task performed the second best among these tasks in the present study.

*Keywords: equiluminance, luminance, luminous efficiency, cone contrast, heterochromatic flicker photometry (HFP), minimum motion (MM), minimally distinct border (MDB)*

## Acknowledgments

We are grateful to Andrew Stockman and Andrew Rider for insightful comments on the manuscript and the diligent and expert work of the reviewers.

This work was supported by National Science Foundation Award BCS-1921771.

Commercial relationships: none.
Corresponding author: Rhea T. Eskew Jr.
Email: r.eskew@northeastern.edu.
Address: Department of Psychology, Northeastern University, Boston, MA, USA.

## Footnote

[1] For the flicker measurements, Sharpe et al. (2005) used a superposition of an approximate D65 background (tritanopically metameric to 566 nm) and the 560-nm standard, which in total produced adaptation that was tritanopically metameric to about 565 nm, at ~1300 Td; we ignore the adapting effects produced by the test lights as the flicker nulls were corrected for that adaptation.

## References

Anstis, S. M., & Cavanagh, P. (1983). A minimum motion technique for judging equiluminance. In J. D. Mollon, & L. T. Sharpe (Eds.), *Colour vision: Physiology and psychophysics* (pp. 155–166). London, UK: Academic Press.

Boynton, R. M. (1978). Ten years of research with the minimally distinct border. In J. C. Armington, J. Krauskopf, & B. R. Wooten (Eds.), *Visual psychophysics and physiology* (pp. 193–207). New York, NY: Academic Press.

Boynton, R. M., Eskew, R. T., Jr., & Olson, C. X. (1985). Blue cones contribute to border distinctness. *Vision Research, 25*(9), 1349–1352, doi:10.1016/0042-6989(85)90053-7.

Boynton, R. M., & Kaiser, P. K. (1968). Vision: The additivity law made to work for heterochromatic photometry with bipartite fields. *Science, 161*(3839), 366–368, doi:10.1126/science.161.3839.366.

Brainard, D. H. (1996). Cone contrast and opponent modulation color spaces. In P. K. Kaiser, & R. M. Boynton (Eds.), *Human color vision* (2nd ed., pp. 563–579). Washington, D.C.: Optical Society of America.

Carroll, J., Neitz, J., & Neitz, M. (2002). Estimates of L:M cone ratio from ERG flicker photometry and genetics. *Journal of Vision, 2*(8), 531–542, doi:10.1167/2.8.1.

Cavanagh, P., MacLeod, D. I., & Anstis, S. M. (1987). Equiluminance: spatial and temporal factors and the contribution of blue-sensitive cones. *Journal of the Optical Society of America A, 4*(8), 1428–1438, doi:10.1364/JOSAA.4.001428.

CIE. (2006). *Fundamental chromaticity diagram with physiological axes - Part 1, Technical Report 170-1:2006*. Vienna, Austria: International Commision on Illumination.

CIE. (2015). *Fundamental chromaticity diagram with physiological axes - Part 2: Spectral luminous efficiency functions and chromaticity diagrams, Technical Report 170-2:2015*. Vienna, Austria: International Commision on Illumination.

Eisner, A., & Macleod, D. I. (1981). Flicker photometric study of chromatic adaption: Selective suppression of cone inputs by colored backgrounds. *Journal of the Optical Society of America, 71*(6), 705–718, doi:10.1364/josa.71.000705.

Eskew, R. T., Jr., McLellan, J. S., & Giulianini, F. (1999). Chromatic detection and discrimination. In K. R. Gegenfurtner, & L. T. Sharpe (Eds.), *Color vision: From genes to perception* (pp. 345–368). Cambridge, UK: Cambridge University Press.

Farnsworth, D. (1943). The Farnsworth-Munsell 100-hue and dichotomous tests for color vision. *Journal of the Optical Society of America, 33*(10), 568–578, doi:10.1364/JOSA.33.000568.

Gibson, K. S., & Tyndall, E. P. T. (1923). Visibility of radiant energy. *Scientific Papers of the Bureau of Standards, 19*, 131–191, doi:10.6028/nbsscipaper.154.

Giulianini, F., & Eskew, R. T., Jr. (1998). Chromatic masking in the (ΔL/L, ΔM/M) plane of cone-contrast space reveals only two detection

mechanisms. *Vision Research, 38*(24), 3913–3926, doi:10.1016/S0042-6989(98)00068-6.

Gunther, K. L., & Dobkins, K. R. (2002). Individual differences in chromatic (red/green) contrast sensitivity are constrained by the relative number of L- versus M-cones in the eye. *Vision Research, 42*(11), 1367–1378, doi:10.1016/S0042-6989(02)00043-3.

Ingling, C. R., Jr., & Martinez, E. (1983). The spatiochromatic signal of the r-g channel. In J. D. Mollon, & L. T. Sharpe (Eds.), *Colour vision: Physiology and psychophysics*. London, UK: Academic Press.

Ingling, C. R., Jr., & Martinez-Uriegas, E. (1983). The relationship between spectral sensitivity and spatial sensitivity for the primate r-g X-channel. *Vision Research, 23*(12), 1495–1500, doi:10.1016/0042-6989(83)90161-X.

Ingling, C. R., Jr., Tsou, B. H. P., Gast, T. J., Burns, S. A., Emerick, J. O., & Riesenberg, L. (1978). The achromatic channel—I. The non-linearity of minimum-border and flicker matches. *Vision Research, 18*(4), 379–390, doi:10.1016/0042-6989(78)90047-0.

Ives, H. E. (1912). XII. Studies in the photometry of lights of different colors. *The London, Edinburgh, and Dublin Philosophical Magazine and Journal of Science, 24*(139), 149–188, doi:10.1080/14786440708637317.

Kaiser, P. K., & Boynton, R. M. (1996). *Human color vision* (2nd ed.). Washington, DC: Optical Society of America.

Kaiser, P. K., Herzberg, P. A., & Boynton, R. M. (1971). Chromatic border distinctness and its relation to saturation. *Vision Research, 11*(9), 953–968, doi:10.1016/0042-6989(71)90215-X.

Kaiser, P. K., Lee, B. B., Martin, P. R., & Valberg, A. (1990). The physiological basis of the minimally distinct border demonstrated in the ganglion cells of the macaque retina. *The Journal of Physiology, 422*(1), 153–183, doi:10.1113/jphysiol.1990.sp017978.

Kleiner, M., Brainard, D. H., & Pelli, D. (2007). What's new in Psychtoolbox-3? *Perception, 36*(Suppl.), 14.

Koenderink, J., van Doorn, A., & Gegenfurtner, K. R. (2018). Color weight photometry. *Vision Research, 151*, 88–98, doi:10.1016/j.visres.2017.06.006.

Kremers, J., Scholl, H. P., Knau, H., Berendschot, T. T., Usui, T., & Sharpe, L. T. (2000). L/M cone ratios in human trichromats assessed by psychophysics, electroretinography, and retinal densitometry. *Journal of the Optical Society of America A, 17*(3), 517–526, doi:10.1364/JOSAA.17.000517.

Lee, B. B., Martin, P. R., & Valberg, A. (1988). The physiological basis of heterochromatic flicker photometry demonstrated in the ganglion cells of the macaque retina. *The Journal of Physiology, 404*(1), 323–347, doi:10.1113/jphysiol.1988.sp017292.

Lennie, P., Pokorny, J., & Smith, V. C. (1993). Luminance. *Journal of the Optical Society of America A, 10*(6), 1283–1293, doi:10.1364/JOSAA.10.001283.

Lindsey, D. T., & Teller, D. Y. (1989). Influence of variations in edge blur on minimally distinct border judgments: a theoretical and empirical investigation. *Journal of the Optical Society of America A, 6*(3), 446–458, doi:10.1364/JOSAA.6.000446.

McLellan, J. S., Goodman, J. B., & Eskew, R. T., Jr. (1994). Achromatic and chromatic detection of mixtures of blobs and isolated edges. *Investigative Ophthalmology & Visual Science, 34*(Suppl.), 1370.

Ripamonti, C., Woo, W. L., Crowther, E., & Stockman, A. (2009). The S-cone contribution to luminance depends on the M- and L-cone adaptation levels: Silent surrounds? *Journal of Vision, 9*(3), 1–16, doi:10.1167/9.3.10.

Rushton, W. A. H., & Baker, H. D. (1964). Red/green sensitivity in normal vision. *Vision Research, 4*, 75–85, doi:10.1016/0042-6989(64)90034-3.

Sharpe, L. T., Stockman, A., Jagla, W., & Jägle, H. (2005). A luminous efficiency function, V*(λ), for daylight adaptation. *Journal of Vision, 5*(11), 948–968, doi:10.1167/5.11.3.

Sharpe, L. T., Stockman, A., Jagla, W., & Jägle, H. (2011). A luminous efficiency function, VD65*(λ), for daylight adaptation: a correction. *Color Research and Application, 36*(1), 42–46, doi:10.1002/col.20602.

Shepard, T. G., Swanson, E. A., McCarthy, C. L., & Eskew, R. T., Jr. (2016). A model of selective masking in chromatic detection. *Journal of Vision, 16*(9), 1–17, doi:10.1167/16.9.3.

Smith, V. C., & Pokorny, J. (1975). Spectral sensitivity of the foveal cone photopigments between 400 and 500 nm. *Vision Research, 15*(2), 161–171, doi:10.1016/0042-6989(75)90203-5.

Smith, V. C., & Pokorny, J. (1995). Chromatic-discrimination axes, CRT phosphor spectra, and individual variation in color vision. *Journal of the Optical Society of America A, 12*(1), 27–35, doi:10.1364/JOSAA.12.000027.

Stockman, A., & Brainard, D. H. (2010). Color vision mechanisms. In M. Bass, C. DeCusatis, J. M. Enoch, V. Lakshminarayanan, G. Li, C. Macdonald, V. Mahajan, . . . E. van Stryland (Eds.),

*OSA handbook of optics: Vol. III. Vision and vision optics* (3rd ed., pp. 11.1–11.104). New York, NY: McGraw-Hill.

Stockman, A., Jagle, H., Pirzer, M., & Sharpe, L. T. (2008). The dependence of luminous efficiency on chromatic adaptation. *Journal of Vision, 8*(16), 1–26, doi:10.1167/8.16.1.

Stockman, A., MacLeod, D. I. A., & Vivien, J. A. (1993). Isolation of the middle-and long-wavelength-sensitive cones in normal trichromats. *Journal of the Optical Society of America A, 10*(12), 2471–2490, doi:10.1364/JOSAA.10.002471.

Stockman, A., & Sharpe, L. T. (2000). The spectral sensitivities of the middle- and long-wavelength-sensitive cones derived from measurements in observers of known genotype. *Vision Research, 40*(13), 1711–1737, doi:10.1016/S0042-6989(00)00021-3.

Stromeyer, C. F., III, Cole, G. R., & Kronauer, R. E. (1987). Chromatic suppression of cone inputs to the luminance flicker mechanism. *Vision Research, 27*(7), 1113–1137, doi:10.1016/0042-6989(87)90026-5.

Stromeyer, C. F., III, Gowdy, P. D., Chaparro, A., Kladakis, S., Willen, J. D., & Kronauer, R. E. (2000). Colour adaptation modifies the temporal properties of the long- and middle-wave cone signals in the human luminance mechanism. *The Journal of Physiology, 526*(Pt 1), 177–194, doi:10.1111/j.1469-7793.2000.t01-1-00177.x.

Vos, J. J. (1978). Colorimetric and photometric properties of a 2° fundamental observer. *Color Research and Application, 3*(3), 125–128, doi:10.1002/col.5080030309.

Wagner, G., & Boynton, R. M. (1972). Comparison of four methods of heterochromatic photometry. *Journal of the Optical Society of America, 62*(12), 1508–1515, doi:10.1364/josa.62.001508.

Wyszecki, G., & Stiles, W. S. (1982). *Color science: Concepts and methods, quantitative data and formulae* (2nd ed.). New York, NY: John Wiley & Sons.

## Appendix A: Theoretical relationship between HFP(λ) and an achromatic mechanism

Under circumstances in which cones adapt independently following Weber's law (von Kries adaptation), and the luminance or achromatic mechanism may be approximated as being a sum of the L and M cone adapted signals, then the achromatic response $\hat{I}$ may be written as

$$\hat{I} = k_1 \frac{\Delta L}{L} + k_2 \frac{\Delta M}{M} \quad \text{(A1)}$$

with the constants being nonnegative. Making the weights relative,

$$I = k \frac{\Delta L}{L} + \frac{\Delta M}{M}, \text{ where } I = \frac{\hat{I}}{k_2} \text{ and } k = \frac{k_1}{k_2} \quad \text{(A2)}$$

The stimulus in question (the "test") produces a cone modulation relative to the adapting condition given by

$$\frac{\Delta L}{L} = \frac{L_{test} - L_{adapt}}{L_{adapt}} = \frac{L_{test}}{L_{adapt}} - 1 \quad \text{(A3)}$$

where $L_{test}$ and $L_{adapt}$ refer to the quantal catch produced in the L cones by the test and the adapting lights, respectively. The M cone contrast is defined similarly.

At equiluminance, the mechanism response is zero, so Equation A2 becomes

$$\frac{\Delta M}{M} = -k \frac{\Delta L}{L} \quad \text{(A4)}$$

which is a straight line with a negative slope $-k$ in the (ΔL/L, ΔM/M) plane of cone contrast space (see Figure 1b).

In a conventional heterochromatic flicker photometry experiment, a monochromatic test light is alternated with a standard light under circumstances in which the S cones contribute little. If we assume that the adapting state is constant across the different test wavelengths—a dubious assumption even with relatively weak tests (Sharpe et al., 2011; Stockman et al., 2008), but one that is often made—then the measured flicker photometric function may be modeled as

$$\hat{HFP}(\lambda) = w_1 L(\lambda) + w_2 M(\lambda) \text{ or,}$$

again making the weights relative,

$$HFP(\lambda) = wL(\lambda) + M(\lambda), \text{ with}$$

$$HFP(\lambda) = \frac{\hat{HFP}(\lambda)}{w_2} \text{ and } w = \frac{w_1}{w_2} \quad \text{(A5)}$$

where now the L and M functions are the (unit peak) cone fundamentals. Note that whereas $k$ (Equation A2) is, under the circumstances defined above, a constant across adapting conditions, $w$ (Equation A5) is not. The relative L and M cone fundamentals contribute

differently depending on the chromatic conditions (Eisner & Macleod, 1981; Sharpe et al., 2011; Stromeyer et al., 2000).

The purpose of this appendix is to show how the weight ($w$) in an HFP function such as $V^*_{D65}(\lambda)$ in Figure 1a is related to the cone contrast weight ($k$) under the limited conditions described above: von Kries adaptation and constant adaptation. We also ignore here possible phase shifts between the cone classes produced by differential adaptation (Stromeyer et al., 1987; Stromeyer et al., 2000).

In heterochromatic flicker photometry, the radiance of the test light is adjusted to minimize the flicker at each test wavelength; thus, the radiance of the test $R(\lambda)$ is inversely proportional to the $HFP(\lambda)$ function (for example, the $V^*_{D65}(\lambda)$ shown in Figure 1a):

$$R(\lambda) = \frac{C}{\mathrm{HFP}(\lambda)} = \frac{C}{wL(\lambda) + M(\lambda)} \quad \text{(A6)}$$

where $C$ is the constant of proportionality. Thus, the effect of each monochromatic test light on the cones is $L_{test} = R(\lambda)L(\lambda)$ and $M_{test} = R(\lambda)M(\lambda)$, and from Equation A4 above we have for the mechanism at equiluminance

$$\begin{aligned} &\frac{\Delta M}{M} = -k\frac{\Delta L}{L} \\ &\frac{R(\lambda)M(\lambda)}{M_{adapt}} - 1 = -k\left[\frac{R(\lambda)L(\lambda)}{L_{adapt}} - 1\right] \\ &R(\lambda)M(\lambda) = -k\frac{M_{adapt}}{L_{adapt}}R(\lambda)L(\lambda) + (k+1)M_{adapt} \\ &R(\lambda) = \frac{(k+1)M_{adapt}}{\left[M(\lambda) + k\frac{M_{adapt}}{L_{adapt}}L(\lambda)\right]} \end{aligned} \quad \text{(A7)}$$

Comparing coefficients in Equations A6 and A7, we see that $C = (k+1)M_{adapt}$ and $w = k(M_{adapt}/L_{adapt})$. This conclusion is analogous to one derived by Stockman et al. (2008) using a different approach.

Thus, in modeling the results of a flicker photometric study by a weighted sum of the L and M cones, the relative L/M weight is given by the relative cone contrast weight ($k$) multiplied by the ratio of the two cone adapting states. The slope of the line in Figure 1b is $-k$; the relative cone weight in Equation 2 and illustrated in Figure 1a is $k$ multiplied by the M-to-L adapting states.

Under the assumptions stated above, the weighting making up the HFP function depends upon the adapting states of the cones; the weighting of the cone contrasts in the *mechanism* does not because the cone contrasts take the adapting states into account.

Note that, although the M adapting state appears in both $C$ and $w$ above and $L_{adapt}$ only appears in $w$, there is nothing privileged about either of the two cone adapting conditions. If instead of casting the problem in terms of the weighting the L cone relative to the M cone as above, we instead begin with the relative weight being on the M cones, then

$$I' = \frac{\Delta L}{L} + k'\frac{\Delta M}{M}, \text{ where } I' = \frac{\hat{I}}{k_1} \text{ and } k' = \frac{k_2}{k_1} = k^{-1} \quad \text{(A1′)}$$

and

$$\begin{aligned} &\mathrm{HFP}'(\lambda) = L(\lambda) + w'M(\lambda), \text{ with } \mathrm{HFP}'(\lambda) \\ &\quad = \frac{\hat{\mathrm{HFP}}(\lambda)}{w_1} \text{ and } w' = \frac{w_2}{w_1} = w^{-1} \end{aligned} \quad \text{(A5′)}$$

$$R'(\lambda) = \frac{C'}{\mathrm{HFP}'(\lambda)} = \frac{C'}{L(\lambda) + w'M(\lambda)} \quad \text{(A6′)}$$

and the same algebra shown above leads to

$$C' = (k'+1)L_{adapt} \quad \text{(A8)}$$

$$w' = k'\frac{L_{adapt}}{M_{adapt}} \quad \text{(A9)}$$

so the L adapting state now appears twice and the M one only once. The point is that the relative weighting of the cone fundamentals in the HFP function is proportional to the relative cone adapting levels.

As noted, von Kries adaptation holds only approximately true under some conditions, and the assumption that the adapting condition does not change across test wavelengths in HFP with monochromatic lights is probably never fulfilled (Stockman et al., 2008).